(Abstract No# (ex: 229)

Application of Electrostatic Tethers for Scattering of Relativistic Particles in the Earth's Radiation Belts

Relativistic Effects on Electrostatic Tethers for Radiation Belt Remediation Applications

Antonio Sanchez-Torres

***Abstract*— An electrostatic tether is a recent technology application for removing energetic particles in Earth's radiation belts. A high voltage source will keep the conductive tether at high positive/negative bias. An effective Coulomb deflection of the particles into the loss cone will produce a high rate of atmospheric penetration, decreasing high-energy particles on radiation belts. The present work focuses on the high, positive-bias case with a thick sheath that must be correctly modeled. For small radius, the tether do collect the relativistic orbital motion limited (OML) current. Relativistic effects modify both potential and density profiles, decreasing the range of the sheath and, in turn, increasing tether current collection. The remediation time increases if relativistic effects are considered. A remediation time of about 5 years is determined for a hundred, 1-MV tethers moving in the same orbit at an altitude of 2000 km. Additionally, the presence of both Coulomb and Lorentz forces may induce thrust or drag on the tether. Both forces are briefly studied with the plasma conditions in the inner radiation belt.**

Keywords—radiation belt remediation; electrostatic tether; relativistic effects; current collection ; orbit motion limited model; sheath

I. INTRODUCTION

High-energy particles trapped in the Van Allen belts remain a constant menace to the operative satellites and manned missions. Several Radiation Belts Remediation (RBR) applications have been studied for years. Wave-injection experiments at the ionosphere have been performed with the High Frequency Active Auroral Research Program (HAARP), which actively generates ELF/VLF radiation for precipitation of the trapped particles in belts [1]. Wave emission of electromagnetic ion cyclotron (EMIC) band from antennas may precipitate particles into the atmosphere [2]. A new application may use space tethers at high bias to effectively scatter the high-energy protons and electrons in the Belts, in the sheath layer produced by them [3]. Tethers electrically floating may be used for scientific application allowing auroral sounding of Earth's ionosphere through secondary electrons emitted by the attracted ion impact against the conductive bare tether [4].

In the present work a cylindrical tether at high-positive bias ϕ_p which effectively deflects protons into the loss cone is considered (see Fig. 1). The tether is immersed in a collisionless, unmagnetized plasma, which is composed of electrons and ions with temperatures T_e and T_i, respectively. Relativistic effects become important if the energy of electrons at rest $m_e c^2$ and $e\phi_p$ are comparable [5]. Potential profiles for a positive tether should be correctly modeled following the relativistic, OML theory for the extremely high potential bias required, which might range from 0.1 to 1 MV, and the plasma conditions within the inner radiation belt. For negative tethers, instead, the characteristic energy $|e\phi_p|$ would be smaller than the energy of ions at rest $m_i c^2$, and relativistic effects would be then negligible. Negative tethers for RBR applications with high-energy electron scattering were considered in [6].

The deflection of energetic protons is studied in order to find the precipitation rate, which will be smaller if relativistic effects become important. However, the electron current collection increases if relativistic effects are considered. Using NASA's AE8/AP8 model of the trapped particle flux, the precipitation rate is determined for a range of altitudes within inner radiation belts.

A single tether requires both Lorentz and Coulomb forces calculations under plasma conditions at final altitudes in Low Earth Orbit (LEO) and initial altitudes in Medium Earth Orbit (MEO). In the altitudes considered both electron density n_∞ and Debye length λ_D varies with the solar flux cycle, normally decreasing and increasing, respectively, with the altitude. Early crude calculations of Coulomb drag on Low Earth Orbit (LEO) satellites at relative motion with respect to the ambient plasma, v_{rel} ($\equiv v_{orb}$ - v_{pl}) , involves satellites in mesothermal flow, i.e. moving subsonic and supersonic with respect to electrons and ions, respectively [7]. Considering a non-tilted, centered magnetic dipole model with a magnetic field B northward, a vertical, electrodynamic tether moving in circular, equatorial orbit will induce drag force for both direct and retrograde orbit. Additionally, passive electrodynamic tether of length L will produce a large potential $v_{rel}LB$ from its motional electric field which naturally feed the tether electric circuit [8]. In an electrostatic application with a cylindrical tether of radius R powered with a High Voltage source, Coulomb forces do produce thrust if the plasma velocity v_{pl} is larger than the orbital velocity v_{orb} [9], whereas it would be

A. Sanchez-Torres is with the Escuela Tecnica Superior de Ingenieros Aeronauticos, Universidad Politecnica de Madrid, Madrid, 28040 Spain (e-mail: antonio.sanchezt@upm.es)

(Abstract No# (ex: 229)

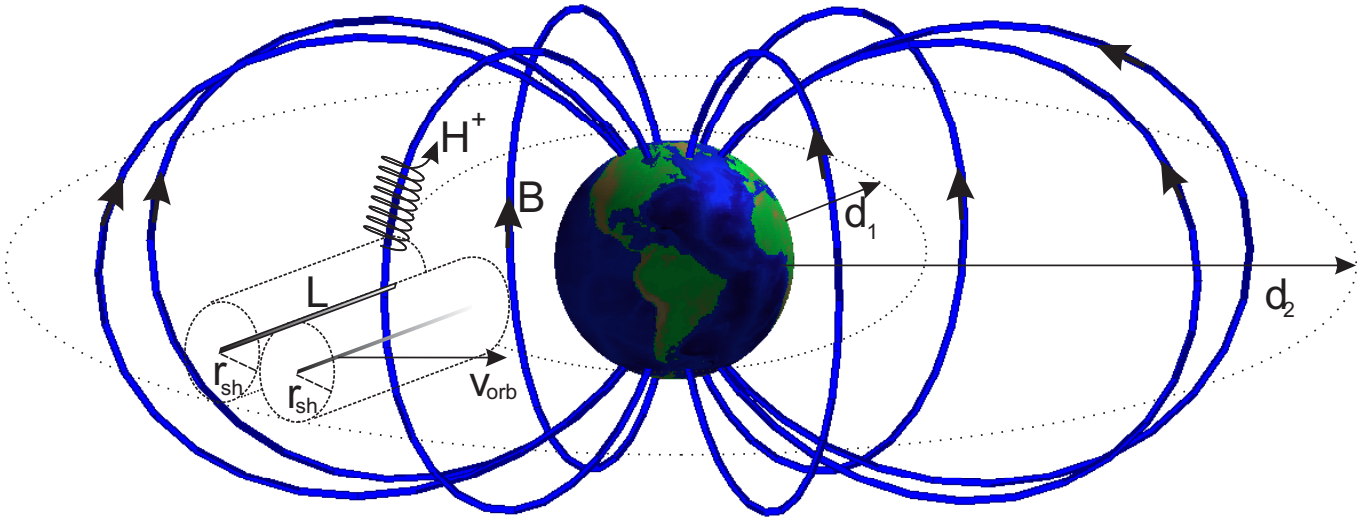

Fig. 1. Description of a vertical, electrostatic tether of length L moving in an equatorial, circular, direct orbit at given altitude $H=(d_1+d_2)/2$. Trapped, charged particles move helicoidally following Earth's magnetic field lines, bouncing back and forth. Several tethers should be considered for faster remediation; two tethers are also shown in the figure.

drag if $v_{rel} \approx v_{orb}$ [10]. The Lorentz force, instead, is thrust for an electrostatic tether. Both forces might be balanced if the tether is not very large and the ratio R/λ_D is very small.

A review of the ambient plasma conditions in the inner radiation belts, i.e. altitudes that ranges from about 2000 to 5000 km, is briefly presented in section II. In section III, numerical results for the relativistic potential profile inside the sheath of the tether is discussed. Both current collection and electrical power required for maintaining tethers at high bias is also discussed. In section IV, we study the forces acting on the tether, showing that both Coulomb and Lorentz forces for a tether might be comparable. The ion scattering problem in that potential profile is studied in section V. In section VI, remediation time is determined for a range of altitudes and protons energies. Finally, conclusions are presented in section VII.

II. Ambient Plasma Conditions In an Circular, Equatorial Orbit

For a circular, equatorial orbit, the orbital velocity at given initial altitude H reads $v_{orb} = \sqrt{\mu_e / a}$, where μ_e is Earth's standard gravitational constant and $a \equiv R_e + H$, being R_e Earth's radius. The plasmasphere does not co-rotate with the Earth, which rotates with an angular velocity of $\Omega_e \approx 7.3 \cdot 10^{-5}$ rad/s; the observed angular velocity for the non-rigid, plasmasphere at $1<a/R_e<4$ is about $0.9\Omega_e$ [11]. The plasma velocity in the equatorial plane is then $v_{pl} \approx 0.42 \cdot a/R_e$. Typical values for the ambient plasma from an altitude H about 2000 km in Earth's equator are $T_e \sim 0.3$ eV, $B \sim 0.14$ G, $n_\infty \sim 700$ cm^{-3}, $v_{rel} \approx v_{orb} \sim 7$ km/s. The prevalent ion species in the range studied here for the plasma is H^+.

As it will be shown in IV section, discussing Coulomb and Lorentz forces involves two lengths, λ_D and v_{rel}/Ω_i, which need be compared to tether radius R and length L, respectively; Ω_i is the ion gyrofrequency, eB/m_i. Both dimensionless ratio $\Omega_i L / v_{rel}$ and λ_D/R will be typically large.

III. Relativistic Potential Profile for a Single Tether

Ion scattering occurs in the sheath of the bare tether. Calculation of the remediation time will be dependent on the sheath model used. We consider the works in [5] and [12] for the relativistic and non-relativistic case, respectively, of positive-bias probe and the numerical method carried out in [13]. The tether is considered at rest in an unmagnetized plasma composed of electrons and ions with temperatures $kT_e \sim kT_i \ll m_e c^2$. Additionally, the assumptions of absence of both trapped electrons and edge effects are considered. The determination of the potential profile requires solving Poisson's equation,

$$\frac{\lambda_D}{r}\frac{d}{dr}\left(r\frac{d}{dr}\frac{e\phi}{kT_i}\right) = \frac{n_e}{n_\infty} - \frac{n_i}{n_\infty}, \qquad (1)$$

with boundary conditions $\phi(r=R)=\phi_p$ and $\phi \to 0$ as $r \to \infty$. Since $e\phi_p \sim m_e c^2 \gg kT_i \sim kT_e$, the normalized ion density $N_i \equiv n_i / n_\infty$ for repelled, positive particles gives the simple Boltzmann law,

$$N_i \approx \exp\left(-\frac{e\phi}{kT_i}\right). \qquad (2)$$

Since $m_e c^2 \gg kT_e$ and considering that the angular momentum J_r is conserved, the normalized electron density, $N_e \equiv n_e / n_\infty$, reads [5]

(Abstract No# (ex: 229)

$$N_e = \left(1+\frac{e\phi}{m_e c^2}\right)^{3/2} \int_0^\infty \frac{dE}{\pi k T_e} \exp\left(-\frac{E}{kT_e}\right) \times \left[2\sin^{-1}\frac{J_r^*(E)}{J_r(E)} - \sin^{-1}\frac{J_R^*(E)}{J_r(E)}\right], \quad (3)$$

where

$$J_r(E) \equiv m_e c r \sqrt{\left[\left(1+\frac{E+e\phi(r)}{m_e c^2}\right)^2 - 1\right]}, \quad (4)$$

$$J_r^*(E) = \min\left\{J_{r'}(E);\quad r' \geq r\right\}. \quad (5)$$

Notice that non-relativistic model is determined with $\beta \equiv e\phi/m_e c^2 = 0$ in the bracket before the integral in (3) and replacing J_r in (3) by $J_r(E) \equiv \sqrt{2m_e r^2\left[E+e\phi(r)\right]}$. The systems equations are numerically solved with an algorithm similar implemented in [13]. The integrand in (3) is carried out with a trapezoidal quadrature algorithm. The method truncates in a finite domain $R \leq r \leq r_{sh}$. The value of the sheath radius r_{sh} is selected for each potential bias ϕ_p value. The potential is discretized with N points not equally spaced. The potential ϕ at the mesh point is found by looking with a Newton method for the zero of a vector-function of components $f_i(\phi) = \phi_i - \tilde{\phi}_i$ and $\phi_i = \phi(r = r_i)$ for $i=0,...,N$. Trying with an initial potential profile ϕ_i, the ion density is calculated with (3), (4) and (5). This readily finds the new potential $\tilde{\phi}_i$ by solving Poisson's equation (4) and imposing boundary conditions, $\tilde{\phi}(R) = \phi_p$ and $\tilde{\phi} \sim 1/r$ at r_{sh}. Density and potential profiles are shown in Figs. 2 and 3, respectively. Both figures shown that the sheath range decreases for the relativistic model given by equations from (1) to (5). Relativistic effects become important for larger ϕ_p values. For ϕ_p=0.1 MV the sheath range is similar for both relativistic and non-relativistic case. Fig. 2 shows that in a broad range from the radius of the tether the electron density do increase for the relativistic case. Fig. 4 shows the variation of the sheath r_{sh} with the ratio $e\phi_p/kT_e$ for several values of R/λ_D. The sheath range increases with the ratios $e\phi_p/kT_e$ and R/λ_D.

Relativistic effects modify the current collection. The OML relativistic current for round wire reads [5],

$$I_{rel} = 2RLecn_\infty \times \sqrt{1+\beta}\sqrt{(1+\beta)^2 - 1}, \quad (6)$$

whereas in the non-relativistic limit $\beta \ll 1$ the current becomes the classical OML formula $I_e = 2RLen_\infty \times \sqrt{2e\phi_p / m_e}$ for electron collection. For $\beta = e\phi_p / m_e c^2 \gg 1$ the current is $I_{urel} = 2RLen_\infty \times \sqrt{2e\phi_p / m_e} \times e\phi_p / \sqrt{2} m_e c^2$. The relativistic model gathers more electrons in a broad range near the tether. The normalized, relativistic electron density at the tether is N_e=0.5×(1+β)$^{3/2}$, whereas in non-relativistic condition is equal to 0.5. The relativistic model increases both OML current collection and electron density at the tether. In addition, the maximum power required $P_{max} \approx I_{OML}\phi_p$ should be very large for the potential values here considered. With typical plasma values and characteristic tether sizes (L=10 km and R=1 mm) the maximum power required would be about 50 kW and 1MW for ϕ_p equal to 0.1 and 1 MV, respectively.

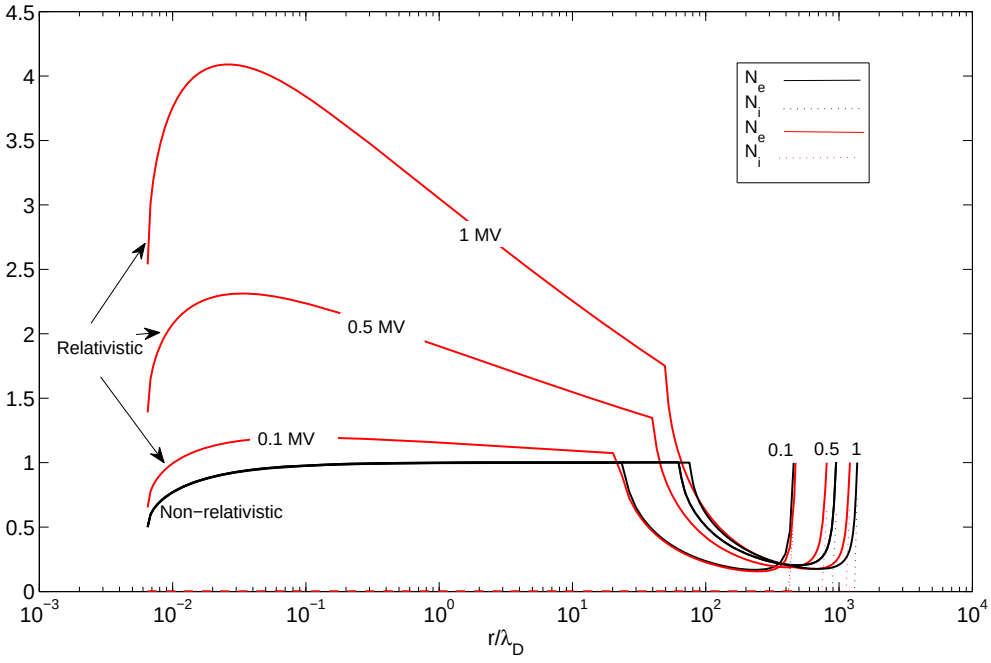

Fig. 2. Relativistic and non-relativistic density profiles at H=2000 km for R =1 mm and ϕ_p = 0.1, 0.5 and 1 MV. For a broad initial range the relativistic model larger N_e values. Notice that $N_e \equiv n_e/n_\infty$ and $N_i \equiv n_i/n_\infty$.

(Abstract No# (ex: 229)

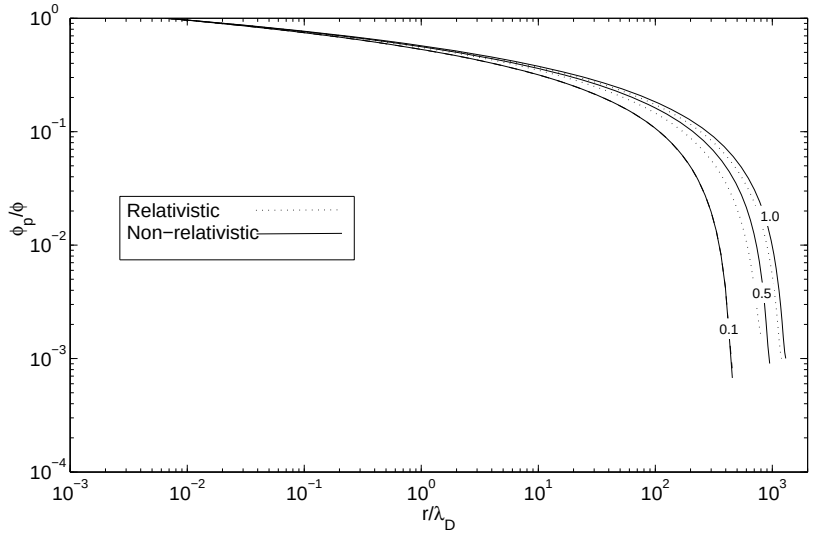

Fig. 3. Relativistic and non-relativistic potential profiles at H=2000 km for R =1 mm and ϕ_p = 0.1, 0.5 and 1 MV. For ϕ_p = 0.1 MV the sheath range is similar for both relativistic and non-relativistic model, whereas the relativistic model modifies the potential structure and reduce the sheath range for larger potentials.

IV. Coulomb-to-Lorentz Force Ratio

In the altitudes here considered the Coulomb force is drag because the nearly Earth's co-rotating plasma does not overtake the tether. Tethers with positive and negative bias ϕ_p allows for drag too. For a positive tether the Coulomb force is made of two contributions to momentum transfer, from electrons that reach the wire, $F_{\rm coll}$, and ions that orbit within the sheath and escape, $F_{\rm orb}$. We will have $F_{orb} \gg F_{coll}$ because the sheath is very large assuming high bias and ratio $\lambda_D / R \gg 1$ and the disparate mass values involved. Further, $F_{\rm coll}$, is just the relativistic OML ion current given in (6) multiplied by the incident momentum per unit charge,

$$F_{coll} = I_{coll} \times \frac{m_e v_{rel}}{e}, \qquad I_{coll} \approx I_{rel}, \tag{7}$$

while the Lorentz force is $F_{\rm L} \sim I_{av} LB$, with the average current I_{av} comparable to I_{coll}. The collected-to-Lorentz force ratio is then

$$\frac{F_{coll}}{F_L} \approx \frac{v_{rel}}{\Omega_i L} \frac{m_e}{m_i} \ll 1. \tag{8}$$

Considering both ion contributions, the Coulomb force can be estimated as proportional to both frontal area and dynamic pressure [9]

$$F_C \propto 2 r_{sh}\ L \times n_\infty\, m_i v_{rel}^2, \tag{9}$$

whereas the Lorentz force on the average current I_{av} reads

$$F_L \sim \frac{1}{2} I_{rel} LB. \tag{10}$$

The Coulomb-to-Lorentz force ratio will then read,

$$\frac{F_C}{F_L} \sim \frac{v_{rel}}{\Omega_i L} \frac{\lambda_D}{R} \frac{r_{sh}}{\lambda_D} \frac{v_{rel}}{c} \frac{1}{\sqrt{1+\beta}\sqrt{(1+\beta)^2 - 1}} \ll 1. \tag{11}$$

For a 10-km tether of radius equal to 1 mm and in the range of altitudes here considered, both ratios $v_{rel}/\Omega_i L$ and v_{rel}/c are very small, and ratios λ_D/R and r_{sh}/λ_D are large. The Coulomb force is then negligible. For much smaller radius R and length L, both Coulomb and Lorentz force might be comparable. The electron current increases if relativistic effects become importatnt and the Lorentz force, in turn, will increase. Additionally, relativistic effects reduce the sheath range, and the Coulomb force, in turn, will decrease.

In the $\phi_p < 0$ case we have the non-relativistic current ($\left| e\phi_p / m_i c^2 \right| \ll 1$) $I_i = 2RLen_\infty \times \sqrt{2e\phi_p / m_i}$ for ion current collection. The Lorentz force on the average current I_{av} is

$$F_L \sim \frac{1}{2} I_i LB = RL \times e n_\infty \sqrt{\frac{2e\phi_p}{m_i}} \times LB, \tag{12}$$

and the Coulomb-to-Lorentz force ratio is then

$$\frac{F_C}{F_L} \sim \frac{v_{rel}}{\Omega_i L} \frac{\lambda_D}{R} \frac{r_{sh}}{\lambda_D} \sqrt{\frac{m_i v_{rel}^2 / 2}{e\left|\phi_p\right|}}. \tag{13}$$

Unlike the positive-bias tether case, Coulomb forces might be larger than Lorentz forces for the $\phi_p < 0$ case.

V. Ion Scattering Calculations

A large number of particles which arrive from the radiation belt should be deflected within the potential of the tether. The scattering of a single particle of mass m_i moving in a field $\phi(r)$ is considered (see Fig. 5). The center of mass of the system is at rest. The deflection angle is $\chi = \pi - 2\delta$, where

$$\delta = \rho \left\{ \int_{r_{\min}}^{r_{sh}} \frac{dr}{r^2 \sqrt{1 - \frac{\rho^2}{r^2} - \frac{e\phi(r)}{E}}} + \int_{r_{sh}}^{r_f} \frac{dr}{r^2 \sqrt{1 - \frac{\rho^2}{r^2} - \frac{e\phi_f}{E}}} \right\}, \tag{14}$$

(Abstract No# (ex: 229)

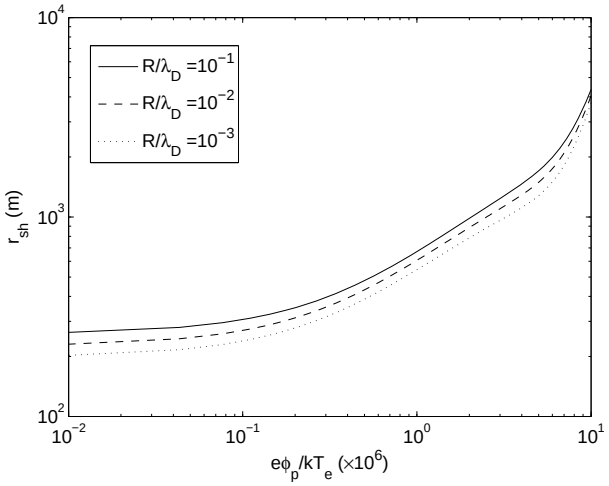

Fig. 4. Variation of the sheath range with the ratio $e\phi_p/kT_e$ for several ratios R/λ_D.

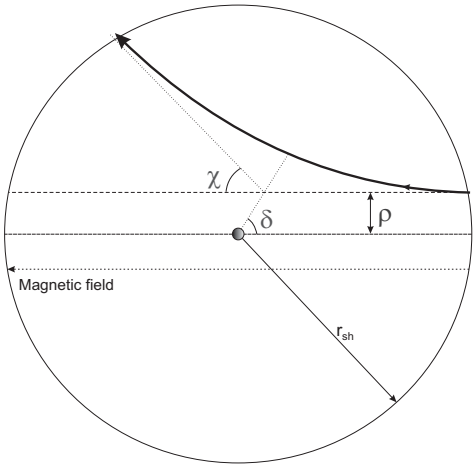

Fig. 5. Ion scattering under the action of the potential generated by a single tether. For symmetry consideration of the ion trajectory in a central field, the deflection angle χ is equal to $\pi+2\delta$.

ρ is the impact parameter, E is the energy of the particle, r_{min}, is the closest approach to the centre, and r_f is the distance for $\phi_f \to 0$. We assume a distance r_f large enough for each potential bias ϕ_p considered. Since $\phi \sim r^{-1}$ at r_{sh}, the potential ϕ_f is equal to $\phi(r_{sh})/(1+r-r_{sh})$. The distance of closest approach, r_{min} , is obtained from equation

$$\frac{\rho^2}{r_{\min}^2}+\frac{e\phi(r_{\min})}{E}=1. \qquad (15)$$

Using polynomial interpolation we obtain an explicit function of $\chi(\rho)$ in the range $0<\rho<r_f$ which will be used in the next section for remediation time determination.

VI. Remediation Time Calculation

Charged particles can be trapped in the magnetic mirrors formed by Earth's magnetic field. For radiation belt remediation the pitch angle between geomagnetic field and velocity of the particle should be reduced. Particles approach the tether spiraling around the magnetic field, which is perpendicular to the tether, with pitch angles distributed between the loss cone angle α_{lc} and $\pi/2$ [6]. Charged particles are effectively scattered into the loss cone if $\alpha_{lc} > \chi > \pi/2$ (see Fig. 6). Considering a non-tilted, magnetic dipole model, the loss cone angle reads

$$\alpha_{lc} = \sin^{-1}\left[\frac{R_e}{a^5}\frac{1}{(4a-3R_e)}\right]^{1/4}. \qquad (16)$$

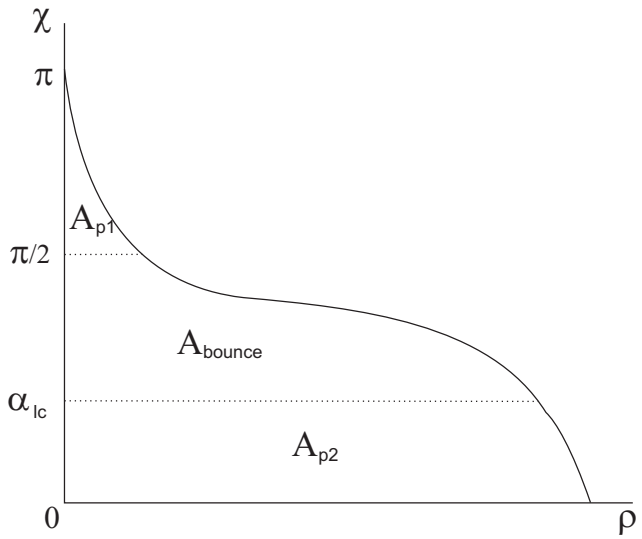

Fig. 6. Scattering angle χ versus impact parameter ρ. Charged particles are effectively scattered into the loss cone if $\alpha_{lc}>\chi>\pi/2$, which is represented by the area $A_{p1}+A_{p2}$.

An estimation of trapped particles in a shell which ranges from d_2 to d_1 is [6]

$$N_{tr} = \frac{F_{tr}(E,a)[\mathrm{m}^{-2}\cdot\mathrm{s}^{-1}]\times\pi\left(d_2^2-d_1^2\right)[\mathrm{m}^2]}{2f_b[\mathrm{s}^{-1}]}, \qquad (17)$$

where F_{tr} is the particle flux given by the NASA's AE8/AP8 family model of trapped particles in Belts. Particles bounce back and forth with a frequency [14],

$$f_b \approx \frac{\sqrt{E/m_i}}{a}\frac{1}{(3.7-1.6\times\sin\alpha_{lc})}. \qquad (18)$$

NASA'S model gives both proton and electron differential flux for a range of energies and altitudes. Fig. 7 shows proton flux versus orbital longitude and a range of energies for an altitude of 2000 km.

The number of deflected protons by the potential of the tethers is

$$\frac{dN_{sc}}{dt} = -2\pi r_{sh} L N_t \times F_{sc}, \qquad (19)$$

where F_{sc} is the deflected flux and N_t is the number of the tethers involved. The trapped proton flux changes for each longitude along the orbit. For a single tether orbiting at some altitude the trapped particle flux reach the sheath for each time

(Abstract No# (ex: 229)

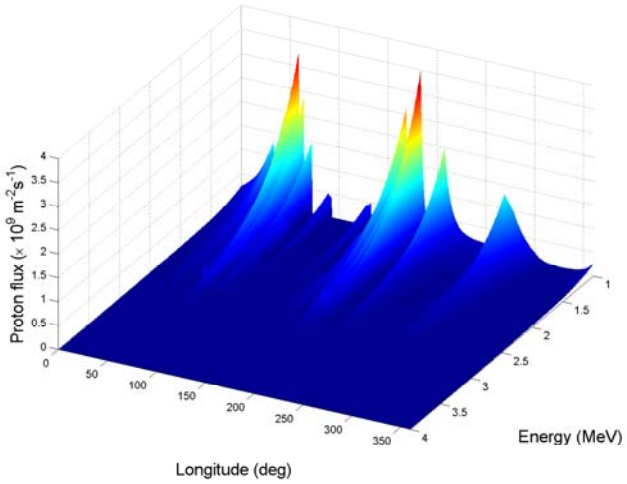

Fig. 7. Proton fluxes at H=2000 km for a range of energies and orbital longitudes.

step $t_{sh}=2r_{sh}/v_{orb}$ for each orbital longitude. The number of deflected particles for each t_{sh} is then

$$N_{sc} = -2\pi r_{sh} L N_t \times F_{sc} \times t_{sh}, \quad F_{sc} \equiv \alpha F_{tr}(E,a), \qquad (20)$$

where α is the deflection efficiency. Charged particles are deflected into the loss cone if $\alpha_{lc} > \chi > \pi/2$, which is represented by the area $A_{p1}+A_{p2}$ in Fig. 6. The deflection efficiency is then

$$\alpha(\chi,\rho) = \frac{\text{Area}(\alpha_{lc} > \chi > \pi/2)}{\text{Area}(0 > \chi > \pi)} = \frac{A_{p1}+A_{p2}}{A_{p1}+A_{p2}+A_{bounce}}. \qquad (21)$$

The remediation time is determined when the number of trapped particles in a shell which ranges from d_2 to d_1 vanishes for a large number of orbits, i.e. the remediation time is found if $N_{tr}+N_{sc}\approx 0$. Fig. 8 shows the remediation time for a single tether moving at given altitude H=2000 km for relativistic and non-relativistic model. Both relativistic and non-relativistic results are similar for ϕ_p=0.1 MV. For larger potential bias values the remediation time increases for all energy ranges if the relativistic model is considered. Results in Fig. 8 for a single tether show that the remediation time is too large for both models. The remediation time would be reduced if the number of tethers N_t moving in the same orbital altitude is increased. With N_t=100, L =10 km and R=1 mm, Figs. 9, 10 and 11 show the remediation time for ϕ_p=0.1, 0.5 and 1 MV, respectively. The distances considered ranges from $1.3R_e$ and to $1.8R_e$. Remediation time will clearly increase if relativistic effects are considered, mainly for larger potential bias.

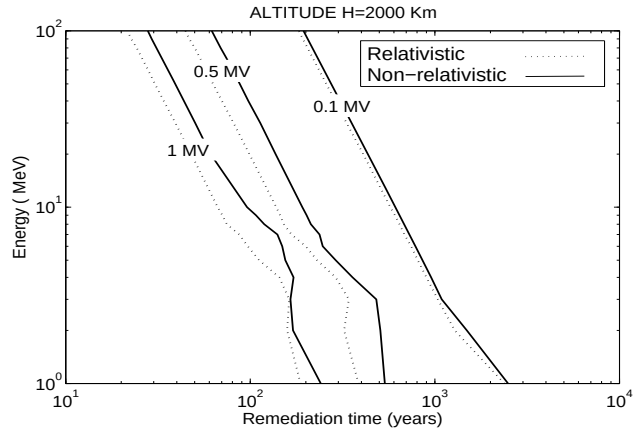

Fig. 8. Remediation time for a single tether moving at given altitude H=2000 km for R =1 mm, ϕ_p = 0.1, 0.5 and 1 MV.

VII. Conclusions

Numerical model of the relativistic potential structure is studied to calculate proton deflection due to a single, positive-bias tether. Since relativistic effects reduce the sheath range r_{sh}, the number of deflected protons N_{sc}, which in turn depends on r_{sh}, will decrease. In the case of negative tethers, electrons will be deflected by a non-relativistic potential structure.

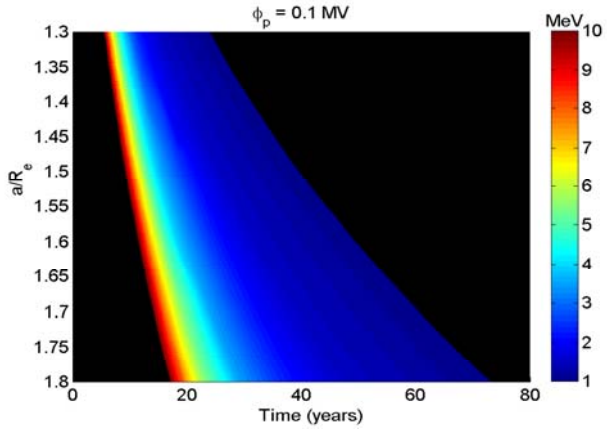

Fig. 9. Remediation time for the relativistic model. Considering 100 tethers moving in the same orbit for L=10 km, R=1 mm and ϕ_p = 0.1 MV.

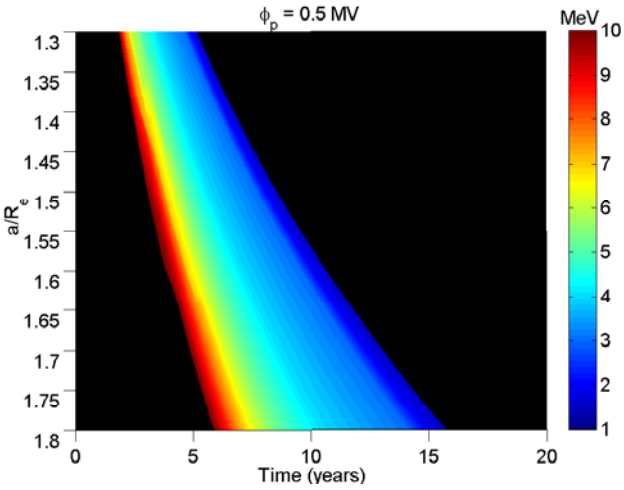

Fig. 10. Remediation time for the relativistic model. Considering 100 tethers moving in the same orbit for L=10 km, R=1 mm and ϕ_p = 0.5 MV.

(Abstract No# (ex: 229)

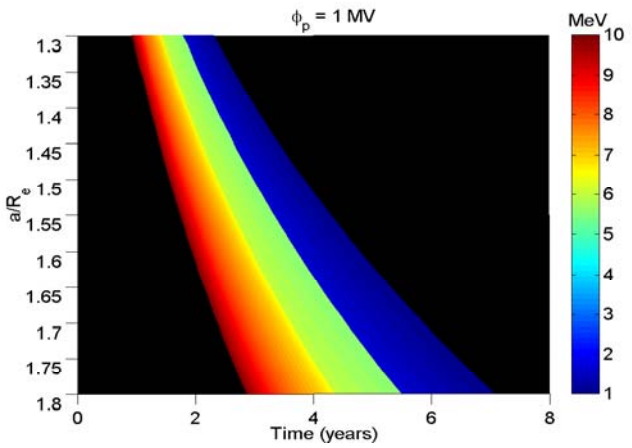

Fig. 11. Remediation time for the relativistic model. Considering 100 tethers moving in the same orbit for L=10 km, R=1 mm and ϕ_p = 1 MV.

For an effective proton remediation application a large number of tethers are needed. Simulation results for a hundred, 1-MV tethers show that the remediation time of an entire 10-km, proton shell would be about 5 years. For simplicity natural losses are not considered in this work. Notice that the remediation time would decrease if natural losses are included.

A problem associated to high-energy particles is their penetration depth in the material of the tether. The collection of particles by the tether then depends on the penetration depth for a range of energies. A positive-bias, aluminum tether of radius R=1mm will effectively collect electrons of energies smaller than 3 MeV (see the Figure 6.4 in [15]). For R values smaller, a wide range of high-energy electrons will not be collected by the tether. For negative tethers of radius R=1mm, protons will be collected if their energies are smaller than 60 MeV.

A more complex structure might be used for RBR application. An electric solar sail (e-sail), which is an array of conductive bare tethers, is a promising application for exploration of the Solar System and satellite de-orbiting [9], [10], [16]. A set of tethers at high potential bias would provide a large virtual area for an effective proton/electron deflection .

ACKNOWLEDGMENT

The author acknowledges NASA's Community Coordinated Modeling Center (CCMC) for the online distribution of the AE-8/AP-8 Radiation Belt model.

REFERENCES

[1] K. Papadopoulos, T. Wallace, G. M. Milikh, W. Peter, and M. McCarrick, “The magnetic response of the ionosphere to pulsed HF heating”, Geophys. Res. Lett., vol. 32, pp. 1-4, 2005.

[2] M. Soria-Santacruz and M. Martinez-Sanchez, “Electronmagnetic Ion Cyclotron Waves for Radiation Belt Remediation Applications”, IEEE Trans. Plasma Sci., vol. 41, pp. 7-22, 2007.

[3] V. V. Danilov, B. A. Elgin, O. S. Grafodatsky, and V. V. Mirnov, “High-Voltage Satellite Tethers For Active Experiments in Space”, Proceedings of the 6th Spacecraft Charging Conference, November 2-6, pp. 165-168, 1998.

[4] J. R. Sanmartin, M. Charro, J. Pelaez, I. Tinao, S. Elaskar, A. Hilgers, and M. Martinez-Sanchez, “Floating bare tether as upper atmosphere probe”, J. Geophys. Res., vol. 111, pp. A11310, 2006.

[5] G. Sanchez-Arriaga and J. Sanmartin, “Relativistic current collection by a cylindrical Langmuir probe”, vol. 19, pp. 063506-1-8, 2012.

[6] R. P. Hoyt and B. M. Minor, “Remediation of Radiation Belts Using Electrostatic Tether Structures”, Proc. IEEE Aerosp. Conf.,Mar. 2005, pp. 583-594.

[7] V. C. Liu, “Ionospheric Gas Dynamic of Satellites and Diagnostic Probes”, Space Sc. Rev., vol. 9, pp. 423-490, 1969.

[8] J. R. Sanmartin, “A review of electrodynamic tethers for science applications”, Plasma Sources Sci. Technol., vol. 19, pp. 1-7, 2010.

[9] A. Sanchez-Torres, “Propulsive Force in an Electric Solar Sail”, Contributions to Plasma Physics, vol. 54, pp. 314-319, 2014.

[10] P. Janhunen, “Simulation study of the plasma brake effect”, Ann. Geophys, unpublished.

[11] B. R. Sandel, J. Goldstein, D. L. Gallagher, andM. Spasojevic, “Extreme ultraviolet imager observations of the structure and dynamics of the plasmasphere”, Space Sci. Rev., vol. 109, pp. 25-46, 2003.

[12] J. R. Sanmartin and R. D. Estes, “The orbital-motion-limited regime of cylindrical Langmuir probes”, Phys. Plasmas, vol. 6, pp. 395-405, 1999.

[13] E. Choiniere and B. E. Gilchrist, “Selfconsistent 2-D kinetic simulations of high-plasma sheaths surronding ion-attracting conductive cylinders in flowing plasmas”, IEEE Trans. Plasma Sci., vol. 41, pp. 3329-3336, 2013.

[14] W. Baumjohann and R. A. Treumann, Basic Space Plasma Physics, Imperial College Press, 1996, pp. 31-46.

[15] D. Hastings and H. Garrett, Spacecraft Environment Interactions, Cambridge Univeristy Press, 1996, pp. 208-215.

[16] P. Janhunen and A. Sandroos, “Simulation study of solar wind push on a charged wire: basis of solar wind electric sail propulsion”, Ann. Geophs.,vol. 25, pp. 755-767, 2007.